Original Article

Galectin-3 promotes calcification of human aortic valve interstitial cells via the NF-kappa B signaling pathway

Jingjing Luo[1#], Shan Wang[2#], Xing Liu[1], Qiang Zheng[1], Zhijie Wang[1], Yuming Huang[3], Jiawei Shi[1]

[1]Department of Cardiovascular Surgery, Union Hospital, Tongji Medical College, Huazhong University of Science and Technology, Wuhan, China; [2]Department of Anesthesiology, Wuhan Children's Hospital, Tongji Medical College, Huazhong University of Science and Technology, Wuhan, China; [3]Department of Thoracic and Cardiovascular Surgery, The First Affiliated Hospital of Nanjing Medical University, Nanjing, China

Contributions: (I) Conception and design: Y Huang, J Shi; (II) Administrative support: J Shi; (III) Provision of study materials or patients: J Shi, Y Huang; (IV) Collection and assembly of data: J Luo, S Wang; (V) Data analysis and interpretation: J Luo, S Wang, Y Huang, X Liu, Q Zheng, Z Wang; (VI) Manuscript writing: All authors; (VII) Final approval of manuscript: All authors.

[#]These authors contributed equally to this work.

Correspondence to: Jiawei Shi. Department of Cardiovascular Surgery, Union Hospital, Tongji Medical College, Huazhong University of Science and Technology, 1277 Jiefang Avenue, Wuhan, China. Email: shijiawei@21cn.com; Yuming Huang. Department of Thoracic and Cardiovascular Surgery, The First Affiliated Hospital of Nanjing Medical University, Nanjing, China. Email: doctor-huangym@foxmail.com.

Background: Calcific aortic valve disease (CAVD) is an active pathobiological process that takes place at the cellular and molecular levels. It involves fibrosis and calcification of aortic valve leaflets, which eventually contributes to heart failure. Galectin-3 (Gal-3), a β-galactoside-binding lectin, is involved in myocardial fibrosis and remodeling. Our study aimed to explore how Gal-3 promoted the osteogenic differentiation of human aortic valve interstitial cells (hVICs) along with elucidating the underlying molecular mechanisms.

Methods: To determine the Gal-3 expression in this study, we included the blood samples and aortic valves (AVs) from patients with CAVD (n=20) and normal controls (n=20). The hVICs were stimulated by Osteogenic medium (OM) and were treated with or without recombinant human Gal-3. Calcified transformation of hVICs was assessed by Alizarin Red S staining and osteogenic gene/protein expression. RNA-sequencing was performed for all different treatments to investigate differentially expressed genes (DEGs) along with exploring the enriched pathways for potential molecular targets of Gal-3. The targets were further detected using Western blotting and immunofluorescence staining.

Results: Gal-3 levels were found to be significantly increased in CAVD patients. Treatment of valve interstitial cells (VICs) with Gal-3 led to a marked increase in Runx2 and ALP-mRNA/protein expression levels as well as calcification. Gene expression profiles of hVICs cultured with or without Gal-3 revealed 79 upregulated genes and 82 down-regulated genes, which were highly enriched in TNF and NF-κB signaling pathways. Furthermore, Gal-3 could activate the phosphorylation of IκBα and interfere with the translocation of p65 into the cell nucleus of hVICs. However, inhibition of this pathway can suppress the osteogenic differentiation by Gal-3.

Conclusions: Gal-3 acts as a positive regulator of osteogenic differentiation by activating the NF-κB signaling pathway in hVICs. Our findings provide novel mechanistic insights into the critical role of Gal-3 in the CAVD progression.

Keywords: Calcific aortic valve disease (CAVD); Galectin-3 (Gal-3); Osteogenesis; NF-kappa B pathway (NF-κB pathway); human aortic valve interstitial cells (hVICs)

Submitted Aug 10, 2021. Accepted for publication Jan 30, 2022.
doi: 10.21037/cdt-21-506
View this article at: https://dx.doi.org/10.21037/cdt-21-506

Introduction

Calcific aortic valve disease (CAVD) is the most common cardiac valvular disease (1), characterized by the active remodeling process of valve mineralization which leads to progressive stenosis of the aortic valve. The pathophysiology of CAVD is an active pathobiological process occurring at the cellular and molecular levels, which involves fibrosis and calcification of aortic valve leaflets causing hemodynamic changes in the heart, eventually contributing to heart failure. Many factors contribute to the pathogenesis of aortic valve calcification, such as endothelial injury, lipid accumulation, inflammatory cytokines, and oxidative stress (2). However, the potential process of ectopic mineralization of the aortic valve remains unclear. So far, no medical treatments have been available to delay or stop the process of CAVD. Conventional cardiovascular drugs being studied in clinical trials have failed to affect disease progression or reduce adverse consequences (3). Therefore, further research is needed to explore the mechanism of disease progression and to identify new treatment targets.

Galectin-3 (Gal-3), a member of the β-galactoside-binding lectin family, has been shown to amplify the inflammatory, profibrotic, and pro-osteogenic responses in several biological processes (4-6). Studies conducted in healthy people and heart failure patients have shown a close relationship between Gal-3, cardiac fibrosis, and heart failure (7-9). Injection of Gal-3 into the pericardial sac leads to inflammation, ventricular remodeling, and cardiac dysfunction in adult male rats (10). Exposure of cardiac fibroblasts to recombinant Gal-3 can result in proliferation, differentiation, and increased collagen production (7). Additionally, Gal-3 could modulate the osteogenic differentiation in vascular smooth muscle cells (VSMC), playing an important role in the development of atherosclerosis (AS). Sádaba *et al.* found an increased Gal-3 level in the aortic valves (AVs) of AS patients, but a deep understanding of its mechanism needs further detection (9).

Therefore, we hypothesized that Gal‐3 could promote AV calcification and regulate osteogenic differentiation in valve interstitial cell (VIC). Furthermore, Gal-3 May be a new biomarker to investigate the severity of aortic valve calcification. We tested this hypothesis using human aortic valvular interstitial cells VICs and blood samples of patients with CAVD. We present the following article in accordance with the MDAR reporting checklist (available at https://cdt.amegroups.com/article/view/10.21037/cdt-21-506/rc).

Methods

Patient population

The study included 20 CAVD patients, whose Doppler echocardiography suggested CAVD (thickness or calcification of aortic valve with or without hemodynamic changes) and CT scan indicated aortic valve calcification (Agatston CT values >130 Hu). Exclusion criteria included rheumatic valvular heart disease, infective endocarditis, Marfan syndrome, severe infectious disease, connective tissue disease, parathyroid disease, renal insufficiency, and other systemic diseases, which affected calcium and phosphorus metabolism. A total of 20 age-matched patients with simple congenital heart disease whose heart Doppler ultrasound and CT did not indicate aortic valve disease were used as the controls. Detailed medical histories were taken from all admitted patients in our center, and venous blood was collected before surgery for routine laboratory testing between February 2019 and December 2019 (*Table 1*).

Human calcified aortic valves were obtained from the above-mentioned patients, who underwent AV replacement. Non-calcified valves were obtained from patients undergoing heart transplantation for their end-stage heart diseases such as myxoma and dilated cardiomyopathy (DCM). Valvular tissues were removed intra-operatively and were divided into three parts, where one part was fixed in formol, one part was placed in high glucose-Dulbecco's Modified Eagle Medium (DMEM) while the other part was stored in liquid nitrogen. This study was approved by the Ethics Committee of Tongji Medical College, Huazhong University of Science and Technology (China) (No. S036). All participants provided written informed consent. The study was conducted in accordance with the Declaration of Helsinki (as revised in 2013).

Cell culture and treatments

Non-calcified valves were rapidly cut into small pieces. After cleaning, they were digested in a medium containing 2 mg/mL type I collagenase for 8–12 h at 37 ℃ in 5% CO_2, shaken at intervals until the tissue was completely digested. Later, the suspension was centrifuged at 1,000 rpm for 5 min, and the separated cells were resuspended and seeded for primary culture in high glucose-DMEM supplemented with 10% fetal bovine serum (FBS, Gibco Laboratories, Gaithersburg, MD), 100 U/mL penicillin (Gibco), and

Table 1 Baseline characteristics of patients

Characteristics	Control (N=20)	CAVD (N=20)	P value
Age (years)	49.80±8.20	54.15±8.01	0.098
BMI (kg/m^2)	22.07±2.45	23.91±3.36	0.055
Male, n (%)	5 [25]	16 [80]	<0.0001
Smoking, n (%)	2 [10]	10 [50]	0.006
Diabetes mellitus, n (%)	1 [5]	1 [5]	1.000
Hypertension, n (%)	6 [30]	8 [40]	0.507
Coronary artery disease, n (%)	2 [10]	5 [25]	0.405
TC (mmol/L)	4.25±0.93	4.53±1.54	0.484
TG (mmol/L)	1.11±0.33	2.22±4.87	0.316
HDL-C (mmol/L)	1.37±0.35	1.20±0.31	0.143
LDL-C (mmol/L)	2.54±0.86	2.67±0.79	0.617
FBG (mmol/L)	4.57±0.51	4.75±1.05	0.492
Hb (g/L)	127.90±16.01	131.2±16.38	0.523
Ca^{2+} (mmol/L)	2.22±0.11	2.20±0.12	0.526
P^{3+} (mmol/L)	1.01±0.21	1.04±0.11	0.651
Gal-3 (ng/mL)	7.63±2.50	9.82±2.58	<0.05
Transvalvular peak velocity (m/s)	1.25±0.21	3.87±1.50	<0.0001
IVS (cm)	0.92±0.16	1.31±0.29	<0.0001
LVEF (%)	64.65±3.80	56.65±9.06	0.001
LVEDD (cm)	4.54±0.46	5.69±0.69	<0.0001

CAVD, calcific aortic valve disease; BMI, body mass index; TC, total cholesterol; TG, triglycerides; HDL-C, high-density lipoprotein cholesterol; LDL-C, low-density lipoprotein cholesterol; FBG, fasting blood glucose; Hb, hemoglobin; Gal-3, galectin-3; IVS, interventricular septal thickness; LVEF, left ventricular ejection fraction; LVEDD, left ventricular end-diastolic diameter.

100 mg/mL streptomycin (Gibco). The cell culture medium was replaced every three days. We used third to fifth-generation cells in all experiments according to the previously described research article (11). The osteogenic medium (OM) included 10 mM β-glycerophosphate, 100 nM dexamethasone, 50 μg/mL vitamin C, 1% FBS, and 100 IU/mL penicillin/streptomycin. Once the cells reached 70–90% confluency, the recombinant human Gal-3, purchased from PeproTech (No.450-38), was added to the cells at a concentration of 2 μg/mL, which was referred to from the previous article (9). BAY 11-7082 was purchased from Selleck (Cat. No. S2913) and dissolved in DMSO to yield a 5nM working solution. Our treatment groups included the Control group (without OM and Gal-3), OM treated group (OM alone), OM plus Gal-3 treated group (OM + Gal-3), and OM plus Gal-3 plus BAY 11-7082 treated group (OM + Gal-3 + BAY 11-7082).

Calcification analysis

The hVICs were seeded into 12-well plates and cultured for 2–3 days until they reached 90% confluency. Cells were then grown for 21 days in the medium described above. Later, Alizarin Red S staining was used to evaluate the degree of cell calcification. Briefly, after 21 days of treatment, the cells were washed thrice with PBS buffer and fixed with 4% paraformaldehyde (PFA) for 10 min. The fixing solution was then discarded, and the cells were again washed thrice with PBS buffer and incubated with 2% Alizarin Red S solution at room temperature for 20 min. After rinsing the cells thrice with distilled water, the calcification was observed under a microscope, and the

images were collected to evaluate the degree of calcification. To quantify the staining, the percentage of Alizarin Red-positive staining area was analyzed by Image J software.

Histological analysis and cell immunostaining assay

The human aortic valves were first fixed in formol for 48 h, dehydrated, and then embedded in paraffin, and finally cut into 4 μm thick sections. For histological analysis, sections were incubated with 3% H_2O_2 at room temperature for 20 min to block endogenous peroxidase. The sections were then rinsed with TBS and blocked with 10% goat serum for 20 min. The primary antibody working solutions of ALP and Gal-3 were added to the slides and incubated overnight at 4 ℃. After rewarming, the slides were rinsed with TBS and incubated with HRP-labeled polymer conjugated to secondary antibodies for 1 h. Next, freshly prepared DAB was added to each section for microscopic observation. The reaction was terminated immediately after the appearance of light brown color under the microscope. For cell immunostaining, the hVICs were cultured with different interventions for 30 min. Cell immunostaining was performed according to the previous protocols (12). The primary antibody used in this study was p65 (CST, 8242s). After incubating with the corresponding secondary antibody, fluorescent microscopy (Zeiss) was used to capture the images.

Quantitative real-time polymerase chain reaction (qRT-PCR) assay

Total RNA was isolated from the hVICs using TRIzol reagent (Invitrogen, Carlsbad, CA, USA). After dissolution, chloroform was added to extract RNA. We used a Nanodrop spectrophotometer to test the quality of all RNA and selected high-quality samples. The cDNA was synthesized from each RNA sample using the Revert Aid first-strand cDNA synthesis kit (Thermo Fisher Scientific, Waltham, MA, USA). Next, the qRT-PCR was performed using 2× SYBR Green Master Mix (Applied Biosystems, Foster City, CA, USA) on the StepOne Plus Thermal Cycler (Bimake, Houston, TX, USA) according to the manufacturer's instructions. All primers were synthesized by Invitrogen. The final data were analyzed by the $2^{-\Delta\Delta Ct}$ method. The following primers were used: *Runx2* forward: 5'-GGCGGGTAACGATGAAAATT-3'; *Runx2* reverse: 5'-GAGGCGGTCAGAGAACAAACTA-3'; *ALP* forward: 5'-GACAAACTGGGGCCTGAGATA-3'; *ALP* reverse: 5'-CTGACTTCCCTGCTTTCTTGG-3'; *GAPDH* forward: 5'-TCAAGAAGGTGGTGAAGCAGG-3'; *GAPDH* reverse: TCAAAGGTGGAGGAGTGGGT-3'; *Gal-3* forward: 5'-GGCCACTGATTGTGCCTTAT-3'; *Gal-3* reverse: 5'-TCTTTCTTCCCTTCCCCAGT-3'.

Western blotting assay

Total proteins were obtained from the aortic valve tissue abrasives and hVIC extracts by lysing the samples in RIPA buffer containing a protease inhibitor cocktail (MCE) using an ultrasonic cell crusher (SCIENTZ, China). We used BCA Protein Assay Kit (Thermo) to quantify the proteins. Next, the protein samples were separated using sodium dodecyl sulfate-polyacrylamide gel electrophoresis (SDS-PAGE) and electroblotted onto 0.22 μm PVDF membranes using a wet protein transfer system. After blocking with 5% non-fat dry milk in 0.05% Tween 20 for 1 h at room temperature, the blotted membranes were incubated with primary antibodies overnight for Runx2 (CST, 8486 s), ALP (R&D, AF2910), Gal-3 (Zenbio, 250013), GAPDH (Proteintech, 60004-1-Ig), IκBα (CST, 4814 s), and p-IκBα (CST, 2859 s) at 4 ℃. Next, the membranes were washed and incubated with corresponding HRP-conjugated secondary antibodies at 37 ℃ for 1 h. Finally, the immunoreactive bands were developed using SuperSignal West Femto Maximum Sensitivity Substrate (Thermo Fisher Scientific), while the images were analyzed by ImageJ software.

Enzyme-linked immunosorbent assay (ELISA)

After the night of admission and at least 8 h of fasting, venous blood was drawn from the subjects by the nurse of the department at 6 am in the next morning. The blood sample was centrifuged at 1,000 ×g for 15 min within 3 h. Samples were immediately aliquoted and stored at –80 ℃. The concentration of Gal-3 was determined using an ELISA Kit (DGAL30) according to the manufacturer's instructions (R&D Systems).

Detection of mRNA profiles

To investigate the changes in cell mRNA profiles among the different treatments performed in this study, we used RNA-sequencing (RNA-seq). TRIzol reagent (Invitrogen, Carlsbad, CA, USA) was used to isolate RNA from the collected cells. Subsequently, isolated RNAs from different treatments were sent to BGI Co., Ltd. (Wuhan, China)

for RNA-seq, which was performed using a BGISEQ-500 instrument. The "R (version 3.5.1)" software was used to identify differential expression genes (DEGs), after which, a Kyoto Encyclopedia of Genes and Genomes (KEGG) pathway enrichment analysis was performed.

Statistical analysis

Continuous variables were expressed as mean ± standard deviation (SD) and compared using an unpaired Student's *t*-test. Categorical variables were expressed as percentages and compared using the chi-square or Fisher's exact probability test. Differences between groups were evaluated using analysis of variance (ANOVA). All semi-quantitative measurements were captured by ImageJ software. Statistical analysis was performed using SPSS software (version 23.0; IBM SPSS Statistics, Armonk, NY, USA). P values <0.05 were considered statistically significant.

Results

Upregulation of GAL-3 in blood and AVs of CAVD patients

To explore the alteration of Gal-3 in patients with CAVD, we first measured the concentration of serum Gal-3 in 20 CAVD patients and 20 control patients (listed in *Table 1* with details of patients' characteristics). Notably, serum Gal-3 concentration in the CAVD group was significantly higher than that in the control group (*Figure 1A*). The expression of the *Gal-3* gene in the human aortic valves of the CAVD group was also higher than that in the control group (*Figure 1B*). Western blotting further confirmed the increased protein levels of Gal-3 and ALP in calcified aortic valves (*Figure 1C,1D*). Later, histological analysis was performed to show that the expression of Gal-3 was significantly increased in human AVs compared to those in the normal tissues, which was consistent with the expression of osteogenesis-specific protein ALP (*Figure 1E*). Hence, our data proved that Gal-3 was upregulated in the valves and blood of CAVD patients compared to that seen in the control patients.

Gal-3 induces osteogenic differentiation of hVICs in vitro

To detect whether Gal-3 induced osteogenic differentiation of hVICs, we used exogenous Gal-3 protein to interfere with hVICs for 72 h. The results indicated upregulation in mRNA and protein expression levels of two osteogenesis-specific markers Runx2 and ALP (*Figure 2A-2C*). Next, we treated hVICs with Gal-3 in an osteogenic medium for 14 days and stained the cells using Alizarin Red S to test calcification. Both the OM and OM + Gal-3 group stained positively for Alizarin Red S, but the OM + Gal-3 group had more calcium nodules compared to the OM group (*Figure 2D,2E*). Also, the cell immunofluorescence staining showed that the expression of ALP was increased in the Gal-3 group compared to that in the control group (*Figure 2F*). These results indicated that Gal-3 could induce osteogenic differentiation of hVICs *in vitro*.

Identification of differentially expressed genes (DEGs) and KEGG pathway enrichment analysis

Following the treatment with Gal-3, we observed 161 DEGs in the hVICs versus control cells, where 79 genes were found to be upregulated while 82 genes were downregulated (*Figure 3A,3B*). Then, the Kyoto Encyclopedia of Genes and Genomes (KEGG) signal pathway enrichment analysis was performed on these 161 DEGs and the results indicated that the DEGs were highly enriched in functions related to cytokine-cytokine receptor interaction, TNF, IL-17, NF-κB, NOD-like receptor signaling pathways, and so on (*Figure 3C*). The analysis of transcriptional factors related to DEGs showed that RELA and NF-κB1 were the top two key transcriptional factors that led to the changes caused by Gal-3 (*Figure 3D*).

Gal-3 promotes osteogenic differentiation of hVICs through the NF-κB signaling pathway

Based on the results of RNA-seq and KEGG pathway enrichment analysis, the NF-κB signaling pathway was selected for further studies. The hVICs were treated with Gal-3 for several durations ranging between 0 and 120 min (0, 30, 60, 120 min), while the phosphorylation level of IκBα was tested using Western blotting. We found that IκBα was rapidly activated at 30 min and then decreased gradually over time (*Figure 4A*). BAY11-7082, the inhibitor of IκBα phosphorylation, was used to block the activation of Gal-3 in the NF-κB pathway. Western blotting results showed that upon stimulation of hVICs by Gal-3 for 30 min, p-IκBα expression increased two-folds compared to the control group. However, BAY11-7082 reversed this function of Gal-3 (*Figure 4B,4C*). Immunofluorescence staining showed that the nuclear translocation of p65 was

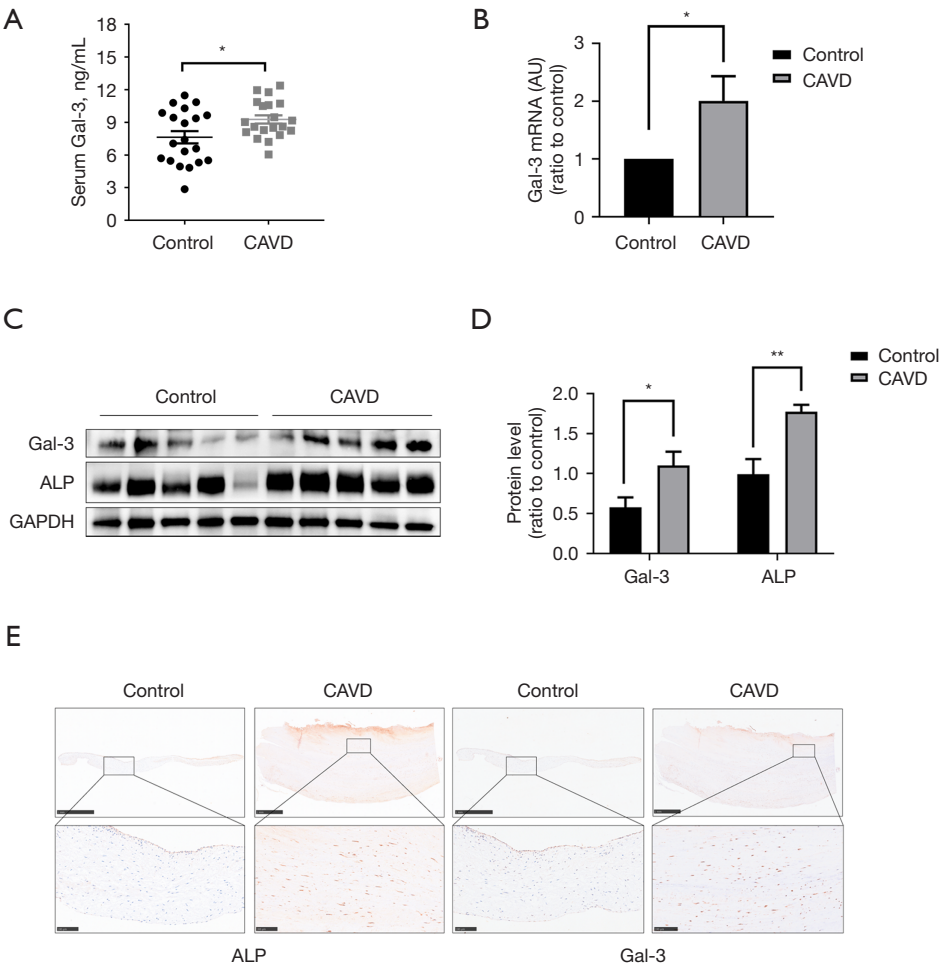

Figure 1 Upregulation of Gal-3 in blood and AVs of CAVD patients. (A) Serum Gal-3 concentration in CAVD and control subjects (n=20); (B) mRNA expression levels of Gal-3 in AVs from CAVD patients and control subjects (n=4); (C) quantification of western blot; (D) protein expression levels of Gal-3 in AVs from CAVD patients and control subjects (n=5); (E) representative pictures of AV sections immunostained for Gal-3 and ALP observed at low (×5, scale bar: 1 mm) and high (×20, scale bar: 100 μm) magnification in controls and CAVD patients. Statistical comparisons were made using Student's *t*-test. All of the data are presented as mean ± SEM. *, P<0.05, **, P<0.01. Gal-3, galectin-3; AVs, aortic valves; CAVD, calcific aortic valve disease.

significantly increased in hVICs after 30 min of Gal-3 treatment compared to that seen in the control group, while BAY11-7082 reversed the nucleation effect of p65 caused by Gal-3 (*Figure 4D*). Next, we detected the expression of ALP and Runx2 in hVICs stimulated with Gal-3 with or without BAY11-7082. Western blotting showed that BAY11-7082 could decrease the expression of ALP and Runx2 led by Gal-3 (*Figure 4E,4F*). The results of immunofluorescence staining were found to be consistent with Western blotting results (*Figure 4G*). Moreover, after culturing the hVICs in OM with or without Gal-3 or BAY11-7082 for 21 days, calcium nodules of hVICs were found to be decreased in the Gal-3 +BAY11-7082 group compared to that in the Gal-3 group (*Figure 4H,4I*). These results revealed that Gal-3 promoted osteogenic differentiation of hVICs by activating the NF-κB signaling pathway.

Discussion

Currently, seeking new potential therapeutic targets of CAVD is one of the hotspots in the basic research of valvular heart disease. Our study showed that Gal-3, which

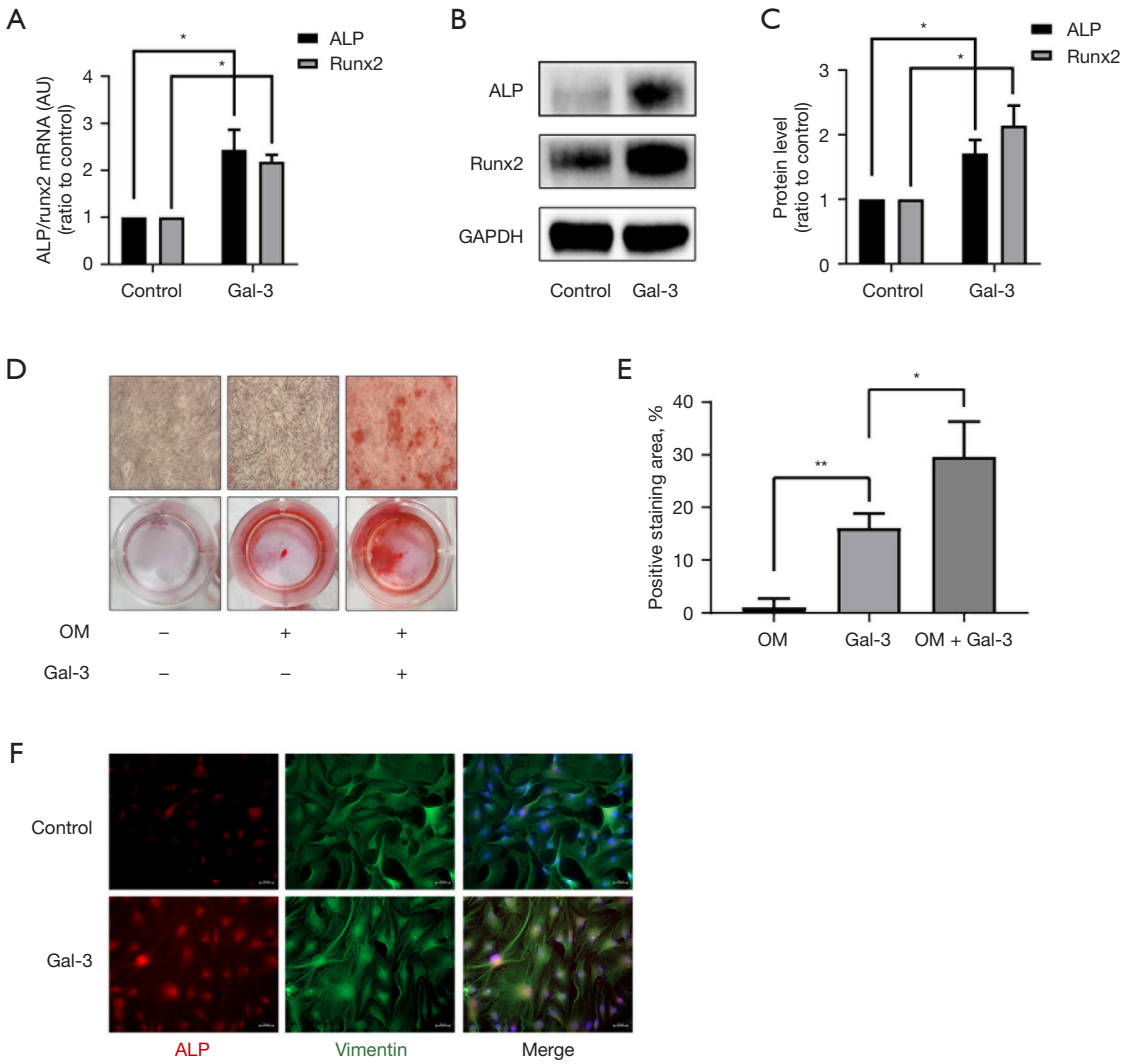

Figure 2 Effect of Gal-3 on calcification-related gene/protein expression and osteogenic differentiation of hVICs. (A) hVICs interfered with or without 2 μg/mL Gal-3 for 72 h, and the mRNA expression levels of ALP and Runx2 detected by qRT-PCR (n=4); (B) Western blotting of Gal-3-treated ALP and Runx2 proteins; (C) quantification of western blot (n=4); (D) Alizarin Red S staining of the cells under different conditioned treatments, including control (normal culture medium), OM (osteogenic medium), and OM + Gal-3 (osteogenic medium with Gal-3 treatment). The microscopic images were taken with the 4× objective; (E) quantification of alizarin red positive area (n=3); (F) immunofluorescent staining was carried out to detect ALP in hVICs treated with or without Gal-3 (scale bar: 50 μm). Statistical comparisons were made using Student's *t*-test. All of the data are presented as mean ± SEM. *, P<0.05, **, P<0.01. Gal-3, galectin-3; hVICs, human aortic valve interstitial cells; qRT-PCR, quantitative real-time polymerase chain reaction.

is highly upregulated in serum and AVs of CAVD patients, serves as a positive regulator of osteogenic differentiation of hVICs, possibly via the NF-κB signaling pathway. The present study verified for the first time that *in vitro* Gal-3 could induce osteogenic differentiation of hVICs through activating the NF-κB signaling pathway. The specific inhibition of this pathway may defer the progression of CAVD caused by Gal-3.

The increased Gal-3 levels in the serum and AVs of AS patients in our study were consistent with the results of the previous study by Sádaba *et al.* (9), who confirmed the correlation between circulating Gal-3 levels and AV calcification. However, the reason why Gal-3 levels were increased in serum during CAVD is not known.

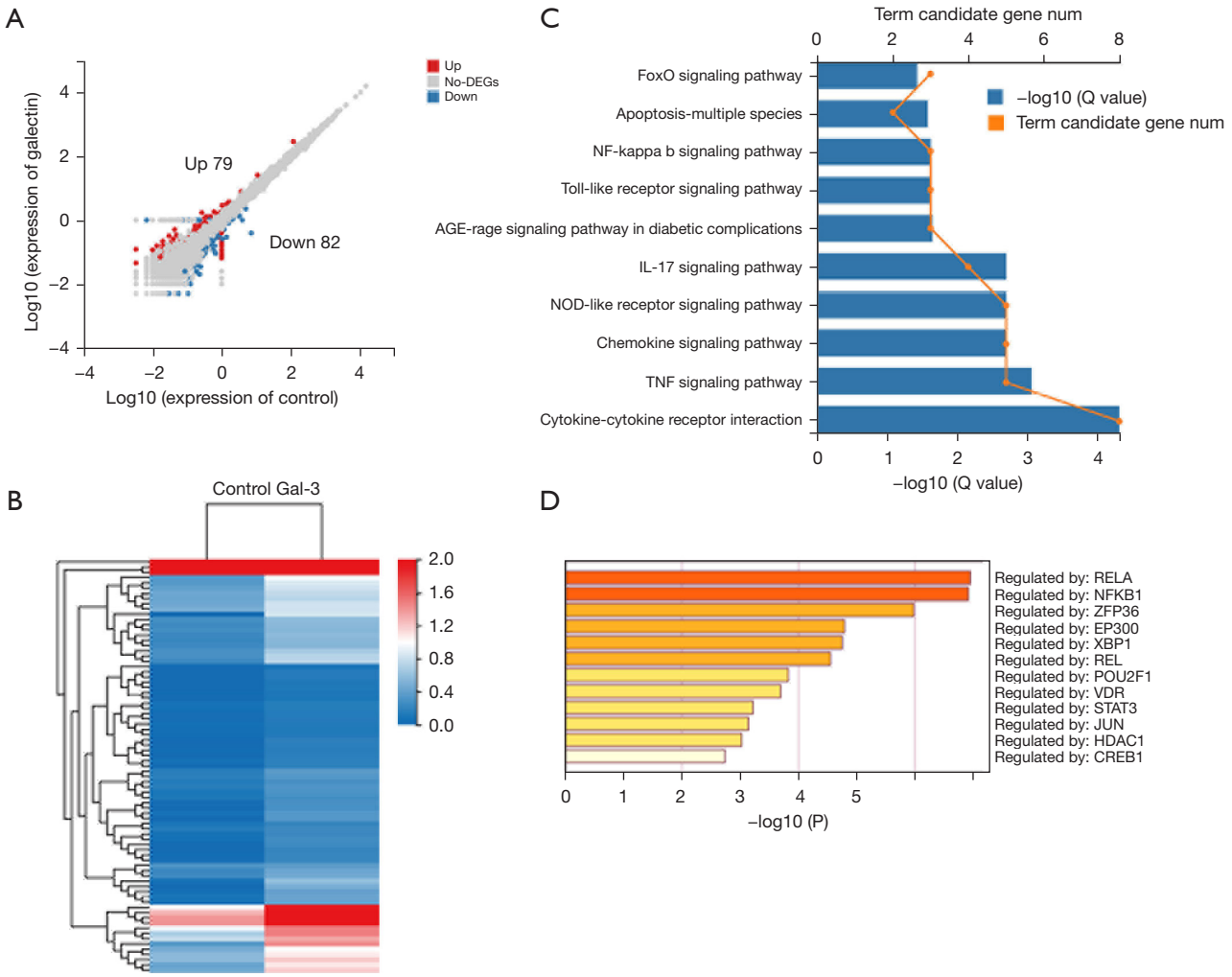

Figure 3 Gene expression profile by RNA-sequencing of hVICs cultured with or without Gal-3. (A) Volcano map of DEGs in C versus Gal-3 [log10 (Gal-3/C); up-regulation: 79 genes and down-regulation: 82 genes]; (B) heatmap for common DEGs with group clusters; (C) KEGG pathway enrichment, where orange dots indicate the degree of enrichment [Q value (–log10)]; (D) transcription factor enrichment, yellow (deep) color indicates the degree of enrichment [Q value (–log10)]. Gal-3, galectin-3; hVICs, human aortic valve interstitial cells; DEGs, differentially expressed genes.

The circulating Gal-3 levels were proven to be positively correlated with cardiac fibrosis and were one of the emerging indicators of the degree of heart failure as per the guidelines. We compared the cardiac structures of different patients through echocardiography, which is shown in *Table 1*. The results indicated that AS patients had lower LVEF values, but thicker interventricular septa along with larger left ventricular end-diastolic diameters. Changes in the cardiac structure due to AS promoted an increased level of Gal-3 in serum, which further promoted aortic valve calcification. Additionally, a higher level of serum Gal-3 before the procedure could predict all-cause mortality of AS patients after the transcatheter aortic valve replacement (TAVR) (13). However, a large-sampled clinical study concluded that Gal-3 levels were not associated with the severity or functional status of AS (14). Calcific aortic stenosis is a disease involving a variety of complex pathological processes and with Gal-3 not being cardiac-specific secretion (15), there is a need for further studies to determine the potential of Gal-3 as a novel biomarker to investigate the severity of aortic valve calcification.

The pathophysiology of CAVD consists of the following

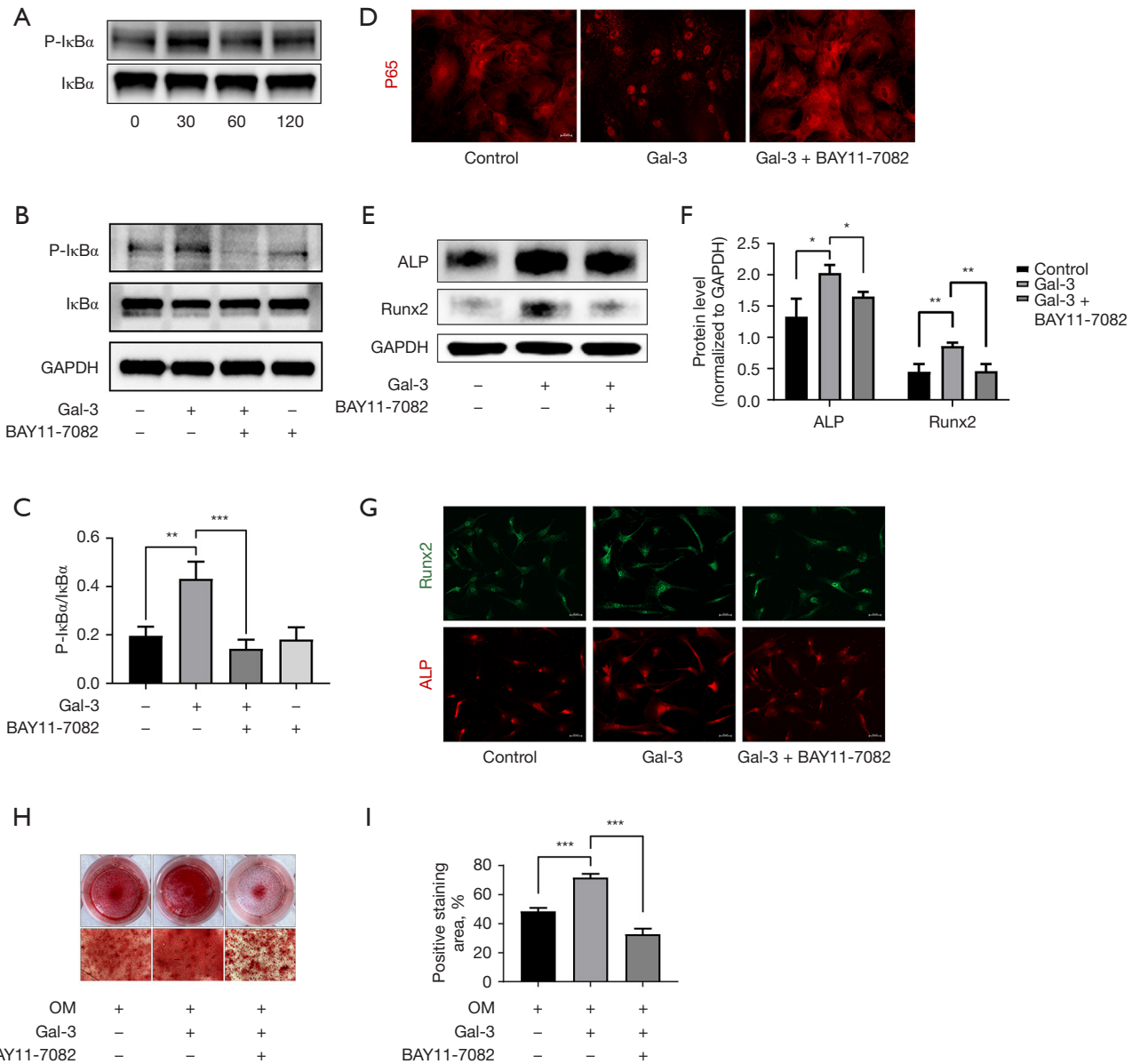

Figure 4 Gal-3 treatment activated NF-κB signaling pathway in hVICs. (A) Western blot analysis revealed the phosphorylation level of IκBα in hVICs treated with Gal-3 for 0, 30, 60, and 120 min; (B) the phosphorylation level of IκBα in hVICs treated with or without Gal-3 or BAY11-7082 for 30 min, assessed by Western blot; (C) quantification of western blot; (D) immunofluorescence of p65 in hVICs treated with or without Gal-3 or BAY11-7082 for 30 min; (E) the protein expression levels of osteogenesis-specific markers (ALP, Runx2) were determined by Western blot in hVICs treated with OM, OM + Gal-3, or OM, Gal-3 + BAY11-7082 for 48 h; (F) quantification of western blot (n=3); (G) the immunofluorescence staining of ALP and Runx2 in AVICs with Gal-3 or Gal-3 + BAY11-7082; (H) representative images of Alizarin Red staining showing calcium deposits in hVICs treated with OM, OM + Gal-3 or OM, Gal-3 + BAY11-7082 for 21 days. The microscopic images were taken with the 4× objective; (I) quantification of alizarin red positive area (n=3). Statistical comparisons were made using Student's *t*-test. All of the data are presented as mean ± SEM. *, P<0.05, **, P<0.01, ***, P<0.001. Gal-3, galectin-3; hVICs, human aortic valve interstitial cells.

two distinct stages: an early initiation phase termed aortic sclerosis and a later propagation phase termed valvular calcification. A previous study indicated that VICs were the main components of the valve leaflet, whose osteogenic phenotype transformation was considered the key part of the above process (16). The osteoblast-like phenotype is characterized by an increased expression of pro-osteogenic biomarkers such as Runx2, ALP, BMPs, and osteocalcin (17-19). In the present study, we demonstrated that Gal-3 induced the increased expression of Runx2 and ALP, clarifying its role in osteogenic differentiation in the aortic valve. As per our findings, Gal-3 has been shown to play a key role in osteoblast differentiation by promoting osteoblastogenesis and suppressing osteoclastogenesis. Also, it is a marker for chondrogenic and osteogenic cell lineages (20). Simon and his colleagues found that Gal-3-deficient ($Lgals3^{-/-}$) mice developed a bone phenotype characterized by reduced trabecular bone compared to that found in the wild-type mice (21). Similarly, in atherosclerosis, Gal-3 was found to transform VSMCs into osteoblast-like cells, contributing to vascular calcification (22). Upregulation of Gal-3 in macrophages promoted the migration of VSMC-derived extracellular vehicles (EVs) to the intima, inducing diabetic vascular intimal calcification (23).

To study the mechanism by which Gal-3 induces hVICs calcification, we used transcriptome sequencing and analyzed the overall gene expression of hVICs following the treatment. The DEGs selected by transcriptome sequencing were highly enriched in TNF, IL-17, NF-κB, NOD-like receptor, and cytokine-cytokine receptor interaction signaling pathways. RELA and NF-κB were found to be the key transcriptional factors in DEGs caused by Gal-3 treatment. The NF-κB signaling pathway has been demonstrated to play an important role in aortic valve calcification (24-26). RELA is the end effector molecule of this pathway, which might be induced by Gal-3. However, a deep understanding of the underlying mechanism needs further exploration. Dina B. AbuSamra and his group members found that Gal-3 could induce the synthesis and secretion of IL-1β through unidentified receptors during corneal repair (27). In CAVD, Gal-3 may also activate the NF-κB signaling pathway through an unidentified receptor.

In our research, Gal-3 was found to induce phosphorylation of IκBα and nuclear translocation of p65, which was reversed by chemical inhibitor BAY11-7082, leading to the attenuation of osteogenic differentiation of VICs. These results confirmed that Gal-3 exerted a significant positive effect on NF-κB activation. Moreover, Gal-3 has also been shown to exert direct modulation of the Wnt/b-catenin signaling pathway, a key event in osteogenic differentiation of VSMCs (24,25). The ERK1/2 pathway was also proven to play an important role in VICs calcification induced by Gal-3. Previous studies have shown that the specific mechanism of action of Gal-3 varies in different cells or tissues. Our research combined with high-throughput sequencing and basic biochemical experiments confirmed that the target of Gal-3 in hVICs could be the NF-κB signaling pathway. However, its potential activation axis still needs further detection.

Our research also had several limitations. Firstly, the control group included patients with simple congenital heart disease, with women making up a large proportion rather than normal healthy people, which might have influenced the results, although the Gal-3 levels did not seem influenced. Secondly, our study had a small number of cases and samples tested for Gal-3 but a larger number of patients may be further required to perform an extensive range of analyses. Also, the specific mechanism underlying Gal-3 activation of NF-κB needs further study. Finally, our study was cross-sectional research and lacked long-term follow-up studies that verified the relationship between Gal-3 and the development and prognosis of CAVD.

Conclusions

This study demonstrated that Gal-3 aggravated the calcification and phenotypical transformation of hVICs by activating the NF-κB signaling pathway. Our findings provide novel mechanistic insights into the critical role of Gal-3 in lagging AV calcification and preventing CAVD.

Acknowledgments

We would like to thank Medgy Technology Co., Ltd. for the help in polishing our paper.
Funding: This study was supported by the National Natural Science Foundation of China (81770387).

Footnote

Reporting Checklist: The authors have completed the MDAR reporting checklist. Available at https://cdt.amegroups.com/article/view/10.21037/cdt-21-506/rc

Data Sharing Statement: Available at https://cdt.amegroups.com/article/view/10.21037/cdt-21-506/dss

Peer Review File: Available at https://cdt.amegroups.com/article/view/10.21037/cdt-21-506/prf

Conflicts of Interest: All authors have completed the ICMJE uniform disclosure form (available at https://cdt.amegroups.com/article/view/10.21037/cdt-21-506/coif). All authors report that this study was supported by the National Natural Science Foundation of China (81770387). The authors have no other conflicts of interest to declare.

Ethical Statement: The authors are accountable for all aspects of the work in ensuring that questions related to the accuracy or integrity of any part of the work are appropriately investigated and resolved. This study was approved by the Ethics Committee of Tongji Medical College, Huazhong University of Science and Technology (China) (No. S036). All participants provided written informed consent. The study was conducted in accordance with the Declaration of Helsinki (as revised in 2013).

References

1. Bonow RO, Leon MB, Doshi D, et al. Management strategies and future challenges for aortic valve disease. Lancet 2016;387:1312-23.
2. Dutta P, Lincoln J. Calcific Aortic Valve Disease: a Developmental Biology Perspective. Curr Cardiol Rep 2018;20:21.
3. Otto CM, Prendergast B. Aortic-valve stenosis--from patients at risk to severe valve obstruction. N Engl J Med 2014;371:744-56.
4. Bäck M, Gasser TC, Michel JB, et al. Biomechanical factors in the biology of aortic wall and aortic valve diseases. Cardiovasc Res 2013;99:232-41.
5. Donato M, Ferri N, Lupo MG, et al. Current Evidence and Future Perspectives on Pharmacological Treatment of Calcific Aortic Valve Stenosis. Int J Mol Sci 2020;21:8263.
6. Wan SY, Zhang TF, Ding Y. Galectin-3 enhances proliferation and angiogenesis of endothelial cells differentiated from bone marrow mesenchymal stem cells. Transplant Proc 2011;43:3933-8.
7. He J, Li X, Luo H, et al. Galectin-3 mediates the pulmonary arterial hypertension-induced right ventricular remodeling through interacting with NADPH oxidase 4. J Am Soc Hypertens 2017;11:275-89.e2.
8. Sharma UC, Pokharel S, van Brakel TJ, et al. Galectin-3 marks activated macrophages in failure-prone hypertrophied hearts and contributes to cardiac dysfunction. Circulation 2004;110:3121-8.
9. Sádaba JR, Martínez-Martínez E, Arrieta V, et al. Role for Galectin-3 in Calcific Aortic Valve Stenosis. J Am Heart Assoc 2016;5:e004360.
10. Blanda V, Bracale UM, Di Taranto MD, et al. Galectin-3 in Cardiovascular Diseases. Int J Mol Sci 2020;21:9232.
11. Ibarrola J, Martínez-Martínez E, Sádaba JR, et al. Beneficial Effects of Galectin-3 Blockade in Vascular and Aortic Valve Alterations in an Experimental Pressure Overload Model. Int J Mol Sci 2017;18:1664.
12. Huang Y, Xu K, Zhou T, et al. Comparison of Rapidly Proliferating, Multipotent Aortic Valve-Derived Stromal Cells and Valve Interstitial Cells in the Human Aortic Valve. Stem Cells Int 2019;2019:7671638.
13. Zhang HL, Song GY, Zhao J, et al. Preprocedural circulating galectin-3 and the risk of mortality after transcatheter aortic valve replacement: a systematic review and meta-analysis. Biosci Rep 2020;40:BSR20202306.
14. Testuz A, Nguyen V, Mathieu T, et al. Influence of metabolic syndrome and diabetes on progression of calcific aortic valve stenosis. Int J Cardiol 2017;244:248-53.
15. Du XJ, Zhao WB, Nguyen MN, et al. β-Adrenoceptor activation affects galectin-3 as a biomarker and therapeutic target in heart disease. Br J Pharmacol 2019;176:2449-64.
16. Di Vito A, Donato A, Presta I, et al. Extracellular Matrix in Calcific Aortic Valve Disease: Architecture, Dynamic and Perspectives. Int J Mol Sci 2021;22:913.
17. Hadji F, Boulanger MC, Guay SP, et al. Altered DNA Methylation of Long Noncoding RNA H19 in Calcific Aortic Valve Disease Promotes Mineralization by Silencing NOTCH1. Circulation 2016;134:1848-62.
18. Rutkovskiy A, Malashicheva A, Sullivan G, et al. Valve Interstitial Cells: The Key to Understanding the Pathophysiology of Heart Valve Calcification. J Am Heart Assoc 2017;6:006339.
19. Rattazzi M, Iop L, Faggin E, et al. Clones of interstitial cells from bovine aortic valve exhibit different calcifying

potential when exposed to endotoxin and phosphate. Arterioscler Thromb Vasc Biol 2008;28:2165-72.
20. Zhou Z, Immel D, Xi CX, et al. Regulation of osteoclast function and bone mass by RAGE. J Exp Med 2006;203:1067-80.
21. Simon D, Derer A, Andes FT, et al. Galectin-3 as a novel regulator of osteoblast-osteoclast interaction and bone homeostasis. Bone 2017;105:35-41.
22. Menini S, Iacobini C, Ricci C, et al. The galectin-3/RAGE dyad modulates vascular osteogenesis in atherosclerosis. Cardiovasc Res 2013;100:472-80.
23. Sun Z, Li L, Zhang L, et al. Macrophage galectin-3 enhances intimal translocation of vascular calcification in diabetes mellitus. Am J Physiol Heart Circ Physiol 2020;318:H1068-79.
24. Liu M, Li F, Huang Y, et al. Caffeic Acid Phenethyl Ester Ameliorates Calcification by Inhibiting Activation of the AKT/NF-κB/NLRP3 Inflammasome Pathway in Human Aortic Valve Interstitial Cells. Front Pharmacol 2020;11:826.
25. Huang Y, Zhou X, Liu M, et al. The natural compound andrographolide inhibits human aortic valve interstitial cell calcification via the NF-kappa B/Akt/ERK pathway. Biomed Pharmacother 2020;125:109985.
26. Xu K, Zhou T, Huang Y, et al. Anthraquinone Emodin Inhibits Tumor Necrosis Factor Alpha-Induced Calcification of Human Aortic Valve Interstitial Cells via the NF-kappa B Pathway. Front Pharmacol 2018;9:1328.
27. AbuSamra DB, Mauris J, Argüeso P. Galectin-3 initiates epithelial-stromal paracrine signaling to shape the proteolytic microenvironment during corneal repair. Sci Signal 2019;12:aaw7095.

Cite this article as: Luo J, Wang S, Liu X, Zheng Q, Wang Z, Huang Y, Shi J. Galectin-3 promotes calcification of human aortic valve interstitial cells via the NF-kappa B signaling pathway. Cardiovasc Diagn Ther 2022;12(2):196-207. doi: 10.21037/cdt-21-506

